

# Supplementary material

## *Catalytic applications of Magnetic nanoparticles functionalized using iridium N-Heterocyclic carbene complexes*

*Diego Iglesias, Sara Sabater, Arturo Azua, Jose A. Mata\**

<sup>a</sup>Departamento de Química Inorgánica y Orgánica, Universitat Jaume I,

Avda. Sos Baynat s/n, 12071, Castellón (Spain)

E-mail: [jmata@uji.es](mailto:jmata@uji.es)

Fax: (+34) 964387522; Tel: (+34) 964387516

**S1.- General Procedures**

**S2.- Electrospray Mass Ionization Mass Spectroscopy (ESI/MS)**

**S3.- High Resolution Mass Spectroscopy (HRMS)**

**S4.- X-Ray Diffraction Studies (Single crystal)**

**S5.- High Resolution Transmission Electron Microscopy (HRTEM) Images**

**S6.- FTIR Spectroscopy**

**S7.- Powder XRD Studies**

**S8.- Pictures of the catalyst separation**

**Table S7.** Comparative catalyst activity in the transfer hydrogenation of acetophenone

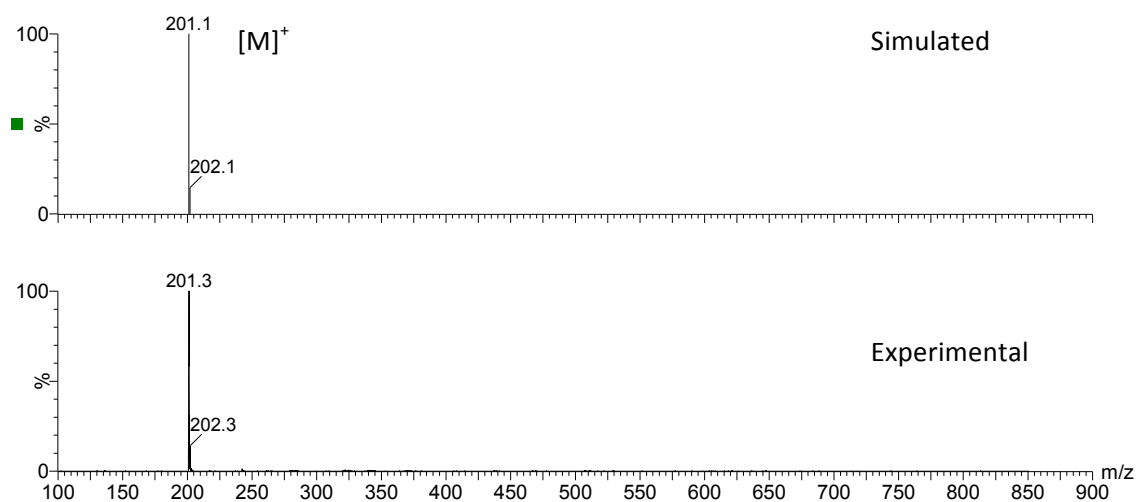
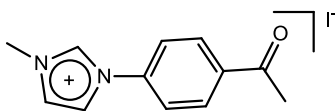
## **S1.- General Procedures**

All manipulations were carried out under aerobic conditions unless otherwise stated. Anhydrous solvents were dried using a solvent purification system (SPS M BRAUN) or purchased from commercial suppliers and degassed prior to use by purging with dry nitrogen and kept over molecular sieves. NMR spectra were recorded on Varian Innova spectrometers operating at 300 or 500 MHz ( $^1\text{H}$  NMR) and 75 and 125 MHz ( $^{13}\text{C}$  NMR), respectively, using  $\text{CDCl}_3$  as solvent at room temperature unless otherwise stated. Elemental analyses were carried out in an EA 1108 CHNS-O Carlo Erba analyzer. Electrospray mass spectra (ESI-MS) were recorded on a Micromass Quatro LC instrument, and nitrogen was employed as drying and nebulizing gas. Infrared spectra (FTIR) were recorded on a JASCO FTIR-6200 spectrometer with a spectral window of 4000-500  $\text{cm}^{-1}$ . High resolution transmission electron microscopy images (HRTEM) and high-angle annular dark-field HAADF-STEM images of the samples were obtained using a Jem-2100 LaB6 (JEOL) transmission electron microscope coupled with an INCA Energy TEM 200 (Oxford) energy dispersive X-Ray spectrometer (EDX) operating at 200 kV. The crystallographic structure of the samples was analyzed by X-ray powder diffraction (XRD) using a Bruker D4-Endeavor diffractometer with a Cu-K radiation with a wavelength of 0.1542 nm. The determination of the metal loading was done by ICP-MS Agilent 7500 CX. The digestion of the samples was carried out under reflux of a mixture of concentrated nitric and hydrochloric acids (3:1) for 12 h. The digestion of the samples after the recycling experiments were carried out after several washes with milli-Q water (10 x 10 mL).

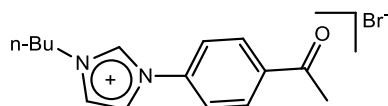
## S2.- Electrospray Mass Ionization Mass Spectroscopy (ESI/MS)

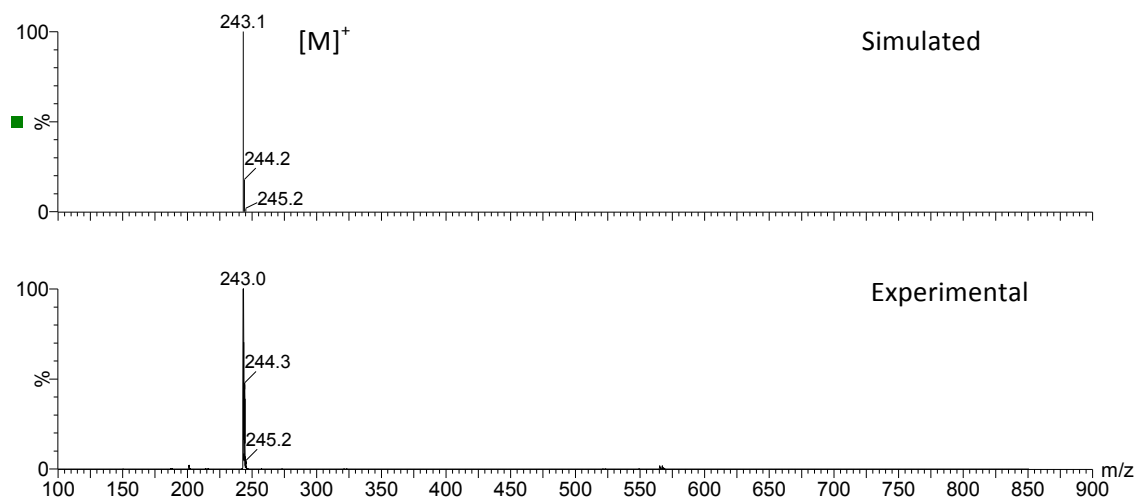
Electrospray mass spectra were recorded on a Micromass Quatro LC instrument using acetonitrile. Nitrogen was employed as drying and nebulising gas.

### S2.1- ESI/MS of the imidazolium salt 1.

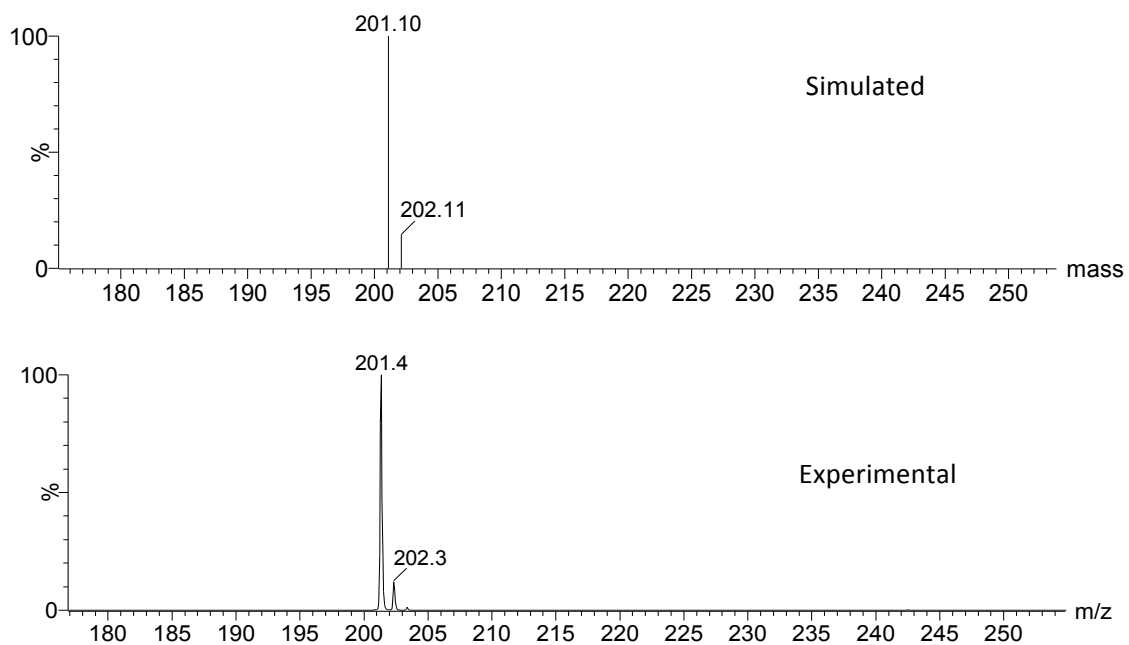
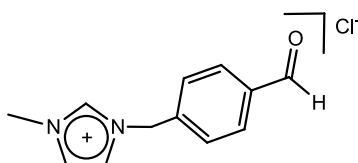


### S2.2- ESI/MS of the imidazolium salt 2.

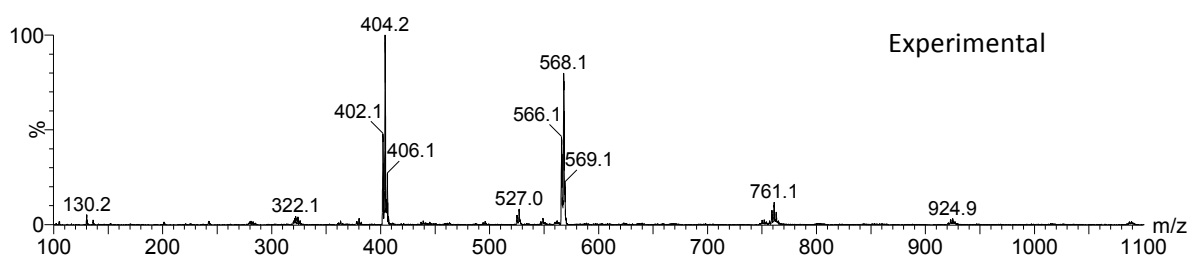
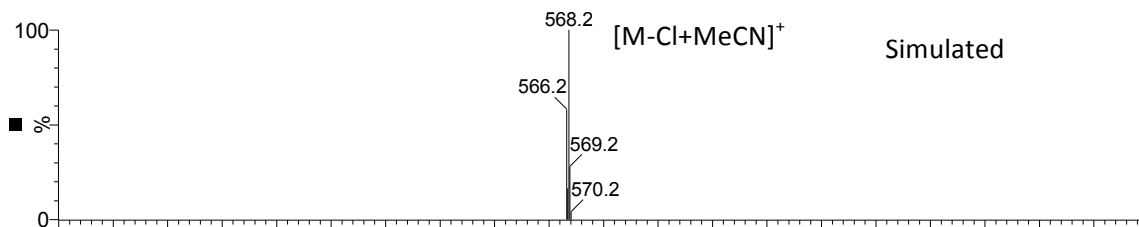
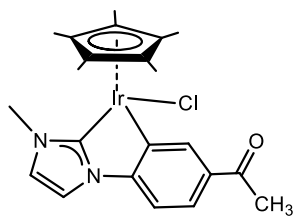




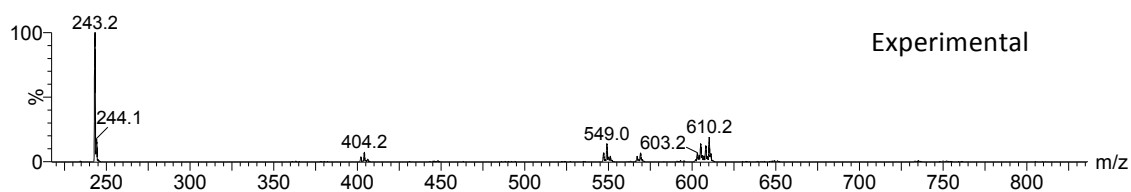
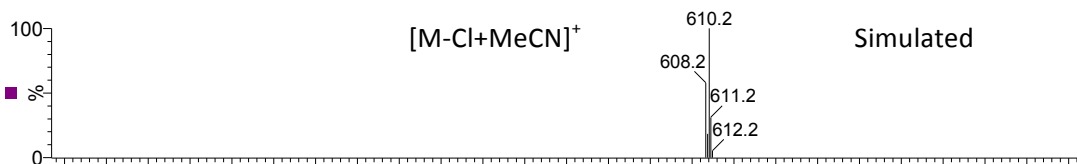
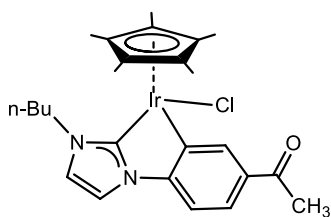
### S2.3- ESI/MS of the imidazolium salt 5.



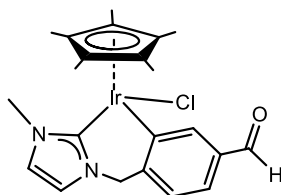
### S2.4- ESI/MS of compound 3

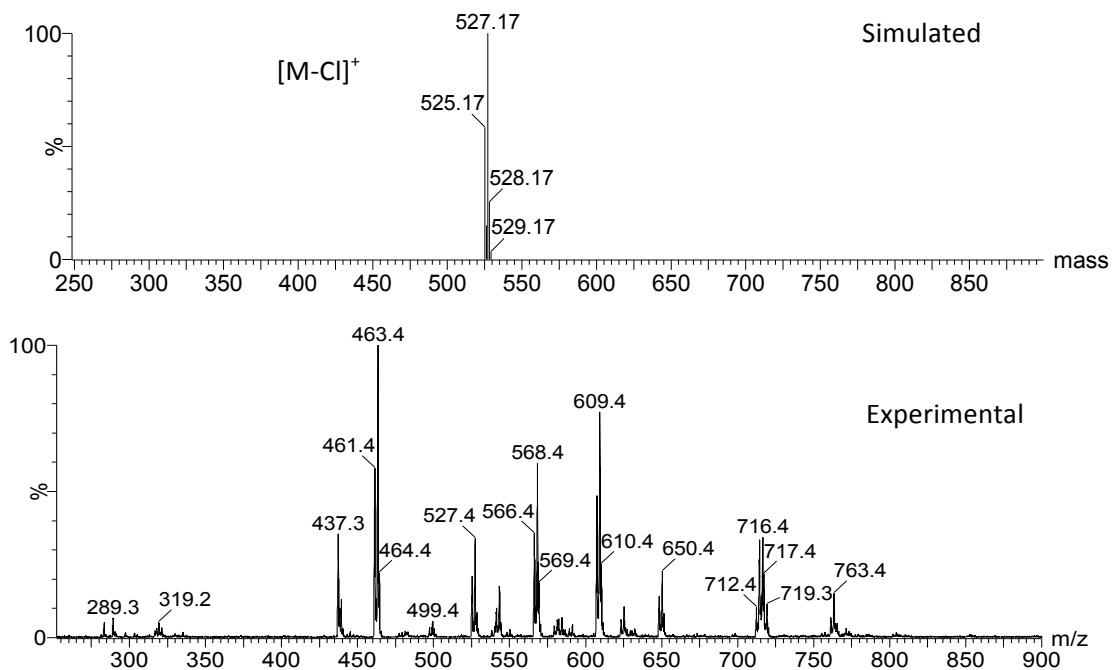


### S2.5- ESI/MS of compound 4



### S2.6- ESI/MS of compound 6



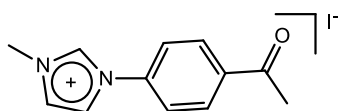


**Electrospray MS (Cone 20V) (m/z, fragments):** 527.4.  $[M-Cl]^+$ , 568.4  $[M-Cl+MeCN]^+$ , 609.4  $[M-Cl+2 MeCN]^+$

### S3.- High Resolution Mass Spectroscopy (HRMS)

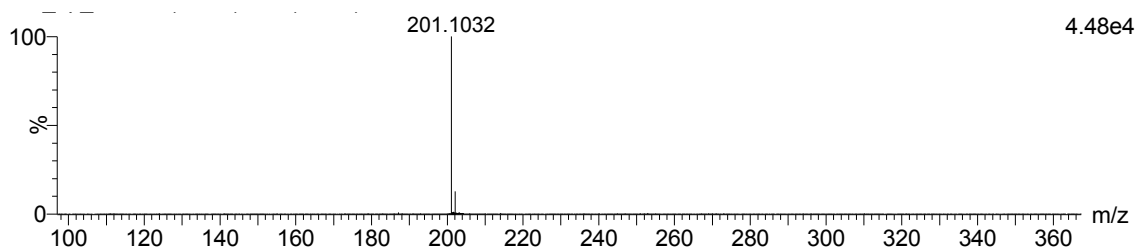
A QTOF I (quadrupole-hexapole-TOF) mass spectrometer with an orthogonal Z-spray-electrospray interface (Micromass, Manchester, UK) was used. The drying gas as well as nebulizing gas was nitrogen at a flow of 400L/h and 80 L/h respectively. The temperature of the source block was set to 120 °C and the desolvation temperature to 150°C. A capillary voltage of 3.5 KV was used in the positive scan mode and the cone voltage was set to 30V. Mass calibration was performed using a solution of sodium iodide in isopropanol:water (50:50) from m/z 150 to 1000 a.m.u. Sample solutions (aprox.  $1 \times 10^{-4}$  M) were infused via syringe pump directly connected to the interface at a flow of 10  $\mu$ l/min. A 1  $\mu$ g/mL solution of 3,5-diiodo-L-tyrosine was used as lock mass.

#### S3.1- HRMS of the imidazolium salt 1



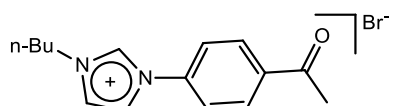
MW = 328.00 g/mol

Fragment: 201.10  $[M - I]^+$



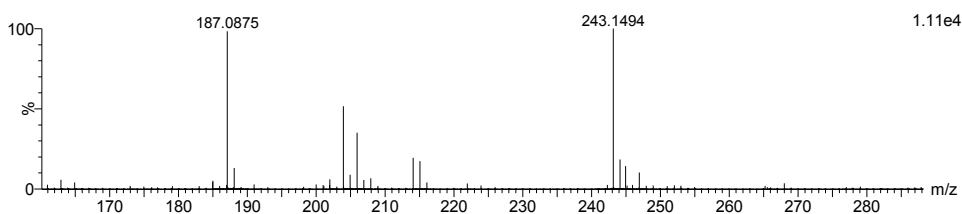
Peak (m/z)	Experimental mass	Theoretical mass	Relative error (ppm)
201.10	201.1032	201.1028	2.0

### S3.2- HRMS of the imidazolium salt 2



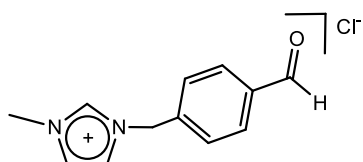
MW = 323.04 g/mol

Fragment: 243.14 [M - Br]<sup>+</sup>



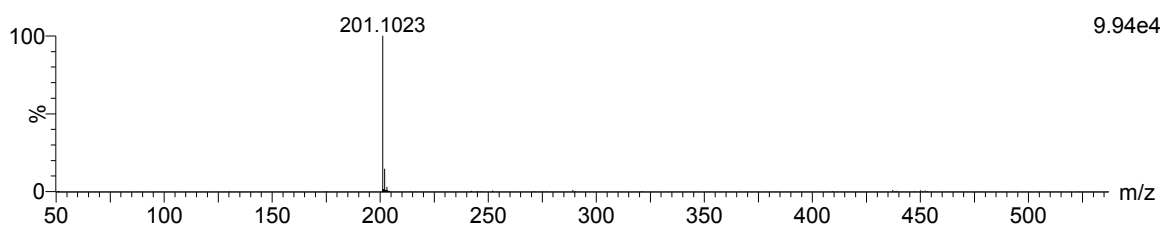
Peak (m/z)	Experimental mass	Theoretical mass	Relative error (ppm)
243.14	243.1494	243.1497	1.2

### S3.3- HRMS of the imidazolium salt 5



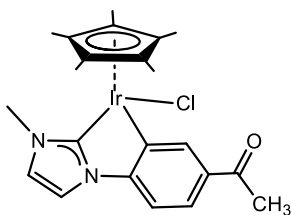
MW = 236.60 g/mol

Fragmento: 201.1023 [M - Cl]<sup>+</sup>



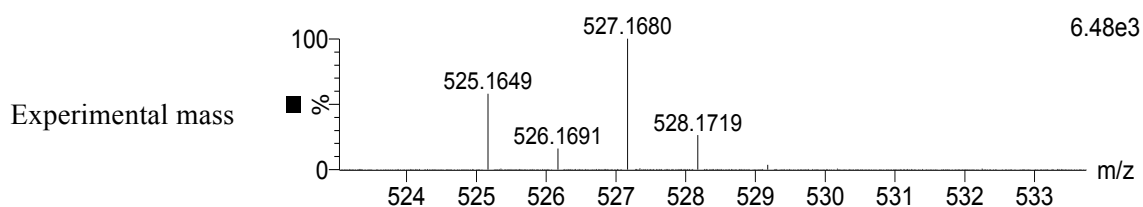
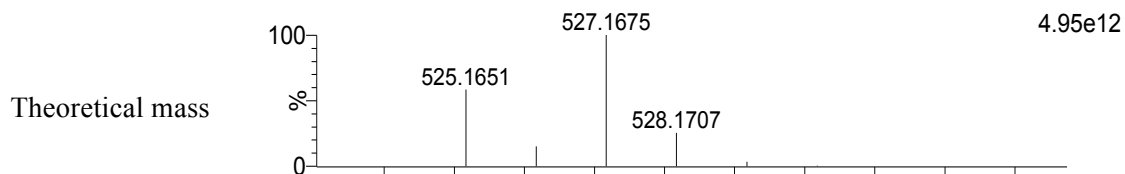
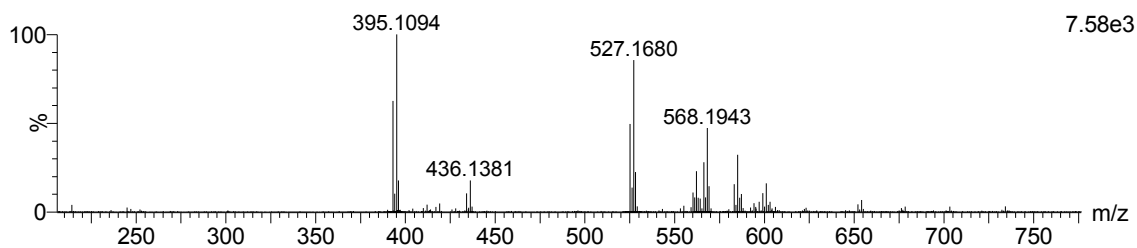
Pico (m/z)	Masa experimental	Masa teórica	Error relativo (ppm)
201.10	201.1023	201.1028	2

### S3.4- HRMS of compound 3



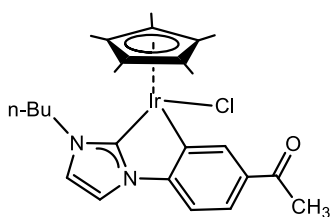
MW = 562.61 g/mol

Fragment: 527.16 [M - Cl]<sup>+</sup>



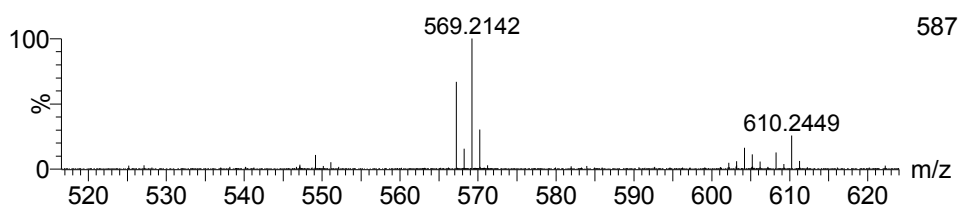
Peak (m/z)	Experimental mass	Theoretical mass	Relative error (ppm)
527.16	527.1680	527.1675	0.9

### S3.5- HRMS of compound 4

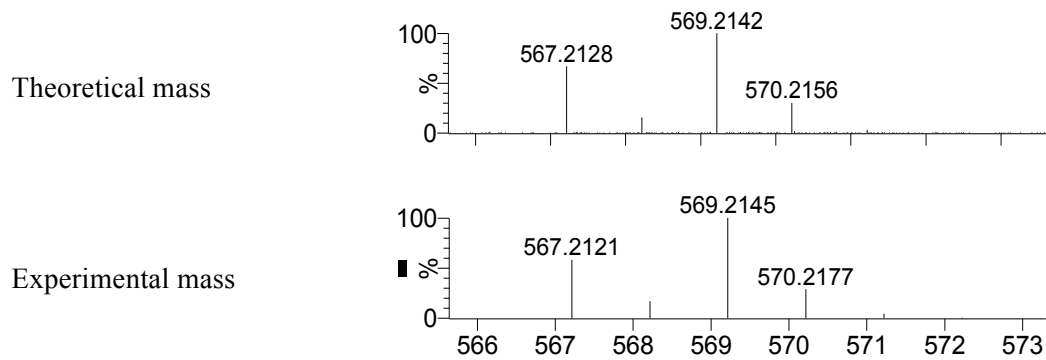


MW = 604.66 g/mol

Fragment: 569.21 [M - Cl]<sup>+</sup>

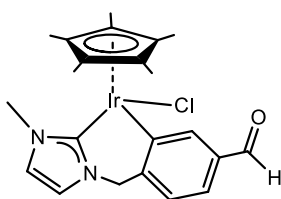






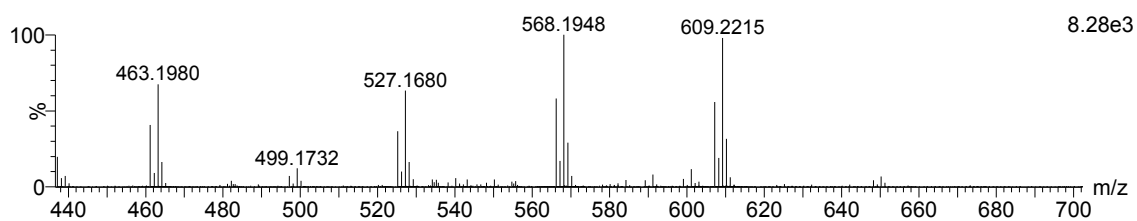
Peak (m/z)	Experimental mass	Theoretical mass	Relative error (ppm)
569.21	569.2145	569.2142	0.5

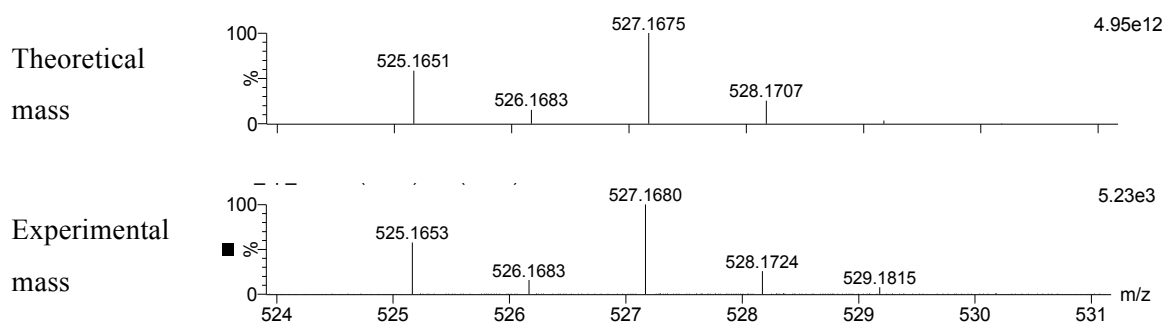
### S3.6- HRMS of compound 6



MW = 562.6 g/mol

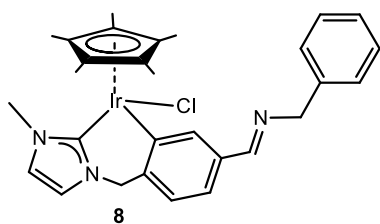
Fragments: 527.2 [M-Cl]<sup>+</sup>,  
 568.2 [M-Cl+MeCN]<sup>+</sup>,  
 609.2 [M-Cl+MeCN+MeCN]<sup>+</sup>





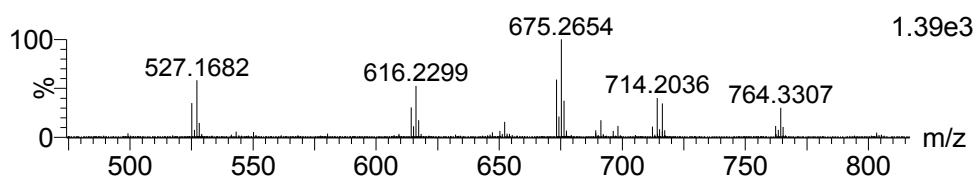
Peak (m/z)	Experimental mass	Theoretical mass	Relative error (ppm)
527.17	527.1680	527.1675	1.0

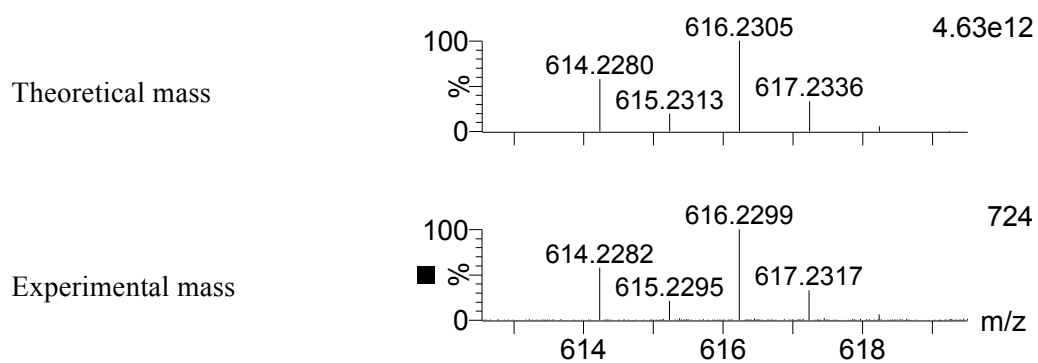
### S3.7- HRMS of the condensation reaction



Fragment: 527.1682  $[M-Cl]^+$  corresponds to complex 6

Fragment: 616.2299  $[M-Cl]^+$  corresponds to complex 8





Peak (m/z)	Experimental mass	Theoretical mass	Relative error (ppm)
616.2	616.2299	616.2305	1.0

#### S4.- X-Ray Diffraction Studies

Crystallographic data and structure refinement for complex **3** (str1513)

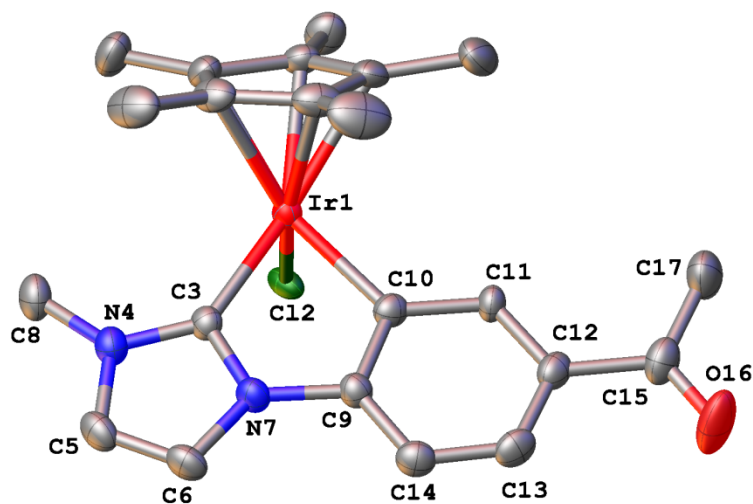


Table S1 Crystal data and structure refinement for **3** (str1513)

Identification code	str1513
Empirical formula	C <sub>22</sub> H <sub>26</sub> ClIrN <sub>2</sub> O
Formula weight	562.10
Temperature/K	200.00(10)
Crystal system	triclinic
Space group	P-1
a/Å	8.4814(3)
b/Å	11.4048(4)
c/Å	11.4291(4)
α/°	96.622(3)
β/°	99.334(3)
γ/°	104.274(3)
Volume/Å <sup>3</sup>	1043.17(6)
Z	2
ρ <sub>calc</sub> /mg/mm <sup>3</sup>	1.790
m/mm <sup>-1</sup>	13.667
F(000)	548.0
Crystal size/mm <sup>3</sup>	0.2443 × 0.0631 × 0.0504
2θ range for data collection	7.94 to 144.4°
Index ranges	-8 ≤ h ≤ 10, -14 ≤ k ≤ 14, -14 ≤ l ≤ 14
Reflections collected	19295
Independent reflections	4047[R(int) = 0.0408]
Data/restraints/parameters	4047/0/251
Goodness-of-fit on F <sup>2</sup>	1.057
Final R indexes [I >= 2σ (I)]	R <sub>1</sub> = 0.0259, wR <sub>2</sub> = 0.0634
Final R indexes [all data]	R <sub>1</sub> = 0.0289, wR <sub>2</sub> = 0.0651
Largest diff. peak/hole / e Å <sup>-3</sup>	1.62/-1.00

Table S2 Fractional Atomic Coordinates (×10<sup>4</sup>) and Equivalent Isotropic Displacement Parameters (Å<sup>2</sup>×10<sup>3</sup>) for **3** (str1513). U<sub>eq</sub> is defined as 1/3 of the trace of the orthogonalised U<sub>ij</sub> tensor.

Atom	x	y	z	U(eq)
Ir1	439.2(2)	2302.93(15)	7811.55(15)	20.96(7)
Cl2	2106.0(12)	2393(1)	9808.0(8)	25.0(2)
N4	-2645(5)	2273(3)	8979(3)	27.7(8)
C10	1160(6)	4178(4)	7937(4)	24.4(9)
C3	-1319(5)	2817(4)	8548(4)	23.0(9)

N7	-1349(5)	4013(3)	8592(3)	25.3(8)
O16	4569(5)	8030(4)	7377(5)	64.1(13)
C9	15(6)	4798(4)	8262(4)	24.4(9)
C24	-224(6)	291(4)	7034(4)	28.1(10)
C26	-1218(6)	914(4)	6348(4)	31.5(10)
C11	2592(6)	4901(4)	7663(4)	23.9(9)
C22	1467(6)	835(4)	6963(4)	27.5(10)
C18	-131(7)	1858(5)	5891(4)	35.6(11)
C20	1540(6)	1774(4)	6240(4)	29.6(10)
C5	-3505(6)	3124(5)	9283(4)	31.2(10)
C23	2924(6)	456(4)	7546(5)	37.1(11)
C17	5560(8)	6319(5)	6905(6)	47.6(14)
C14	222(6)	6048(4)	8284(4)	28.8(10)
C12	2826(6)	6165(4)	7659(4)	28(1)
C15	4329(7)	6926(4)	7320(5)	35.6(11)
C6	-2705(6)	4207(4)	9049(4)	30.2(10)
C13	1630(6)	6725(4)	7971(4)	30.2(10)
C8	-2975(6)	1032(4)	9265(5)	34.7(11)
C21	3044(8)	2465(5)	5838(5)	46.9(14)
C25	-786(7)	-796(4)	7633(6)	43.6(13)
C27	-3074(7)	602(6)	6067(5)	48.2(15)
C19	-678(9)	2665(6)	5049(5)	56.0(17)

Table S3 Anisotropic Displacement Parameters ( $\text{\AA}^2 \times 10^3$ ) for **3** (str1513). The Anisotropic displacement factor exponent takes the form:  $2\pi^2[h^2a^{*2}U_{11} + \dots + 2hka \times b \times U_{12}]$

Atom	$U_{11}$	$U_{22}$	$U_{33}$	$U_{23}$	$U_{13}$	$U_{12}$
Ir1	19.47(11)	19.23(10)	25.11(10)	4.12(6)	6.48(7)	5.41(7)
Cl2	17.6(5)	35.9(5)	20.4(4)	-2.4(4)	4.4(4)	7.7(4)
N4	25(2)	28.6(19)	30.2(19)	7.0(15)	7.7(16)	5.5(16)
C10	29(2)	21(2)	24(2)	5.5(16)	5.5(18)	7.8(18)
C3	19(2)	23(2)	26(2)	3.4(16)	3.6(17)	4.7(17)
N7	22(2)	26.4(18)	30.0(19)	5.2(15)	8.2(15)	9.4(15)
O16	46(3)	28.2(19)	124(4)	29(2)	26(3)	6.5(18)
C9	23(2)	25(2)	27(2)	6.0(17)	6.7(18)	7.8(18)
C24	26(3)	20(2)	37(2)	-0.4(18)	10(2)	3.8(18)
C26	23(3)	34(2)	32(2)	-7.0(19)	-1.4(19)	9(2)
C11	20(2)	21(2)	30(2)	7.2(16)	7.3(18)	2.5(17)

C22	29(3)	22(2)	32(2)	-1.8(17)	7.7(19)	8.2(18)
C18	49(3)	35(3)	26(2)	1.7(19)	5(2)	21(2)
C20	40(3)	24(2)	27(2)	-0.4(17)	16(2)	9(2)
C5	21(2)	43(3)	31(2)	5(2)	8.5(19)	10(2)
C23	31(3)	30(2)	53(3)	7(2)	9(2)	12(2)
C17	48(4)	36(3)	63(4)	14(3)	27(3)	4(3)
C14	29(3)	28(2)	31(2)	5.2(18)	5.8(19)	13(2)
C12	33(3)	22(2)	26(2)	6.6(17)	5.8(19)	3.0(19)
C15	34(3)	28(2)	43(3)	14(2)	6(2)	3(2)
C6	26(3)	38(2)	32(2)	3.8(19)	9.2(19)	16(2)
C13	37(3)	21(2)	33(2)	7.5(17)	3(2)	10.3(19)
C8	25(3)	36(3)	43(3)	12(2)	10(2)	3(2)
C21	64(4)	35(3)	50(3)	7(2)	37(3)	10(3)
C25	39(3)	23(2)	68(4)	6(2)	20(3)	2(2)
C27	26(3)	54(3)	55(3)	-14(3)	-3(2)	10(3)
C19	85(5)	63(4)	32(3)	16(3)	10(3)	39(4)

Table S4 Bond Lengths for **3** (str1513).

Atom	Atom	Length/Å	Atom	Atom	Length/Å
Ir1	C12	2.4583(10)	C9	C14	1.390(6)
Ir1	C10	2.055(4)	C24	C26	1.428(7)
Ir1	C3	2.000(4)	C24	C22	1.436(7)
Ir1	C24	2.259(4)	C24	C25	1.498(7)
Ir1	C26	2.194(4)	C26	C18	1.441(7)
Ir1	C22	2.264(4)	C26	C27	1.498(7)
Ir1	C18	2.142(5)	C11	C12	1.407(6)
Ir1	C20	2.244(4)	C22	C20	1.421(6)
N4	C3	1.341(6)	C22	C23	1.490(7)
N4	C5	1.396(6)	C18	C20	1.439(7)
N4	C8	1.458(6)	C18	C19	1.504(7)
C10	C9	1.406(6)	C20	C21	1.496(7)
C10	C11	1.393(6)	C5	C6	1.333(7)
C3	N7	1.365(5)	C17	C15	1.495(8)
N7	C9	1.411(6)	C14	C13	1.377(7)
N7	C6	1.393(6)	C12	C15	1.490(7)
O16	C15	1.218(6)	C12	C13	1.396(7)

Table S5 Bond Angles for **3** (str1513).

Atom	Atom	Atom	Angle/°	Atom	Atom	Atom	Angle/°
C10	Ir1	C12	91.98(12)	C14	C9	N7	123.8(4)
C10	Ir1	C24	160.54(17)	C26	C24	Ir1	68.8(2)
C10	Ir1	C26	129.52(18)	C26	C24	C22	106.8(4)
C10	Ir1	C22	130.97(18)	C26	C24	C25	128.3(5)
C10	Ir1	C18	97.64(18)	C22	C24	Ir1	71.7(2)
C10	Ir1	C20	99.60(17)	C22	C24	C25	124.7(4)
C3	Ir1	C12	91.17(12)	C25	C24	Ir1	128.6(3)
C3	Ir1	C10	77.44(18)	C24	C26	Ir1	73.8(3)
C3	Ir1	C24	114.47(17)	C24	C26	C18	108.3(4)
C3	Ir1	C26	97.41(18)	C24	C26	C27	126.7(5)
C3	Ir1	C22	151.15(17)	C18	C26	Ir1	68.6(3)
C3	Ir1	C18	114.96(19)	C18	C26	C27	124.9(5)
C3	Ir1	C20	152.95(18)	C27	C26	Ir1	126.4(3)
C24	Ir1	C12	102.68(13)	C10	C11	C12	121.4(4)
C24	Ir1	C22	37.01(17)	C24	C22	Ir1	71.3(2)
C26	Ir1	C12	138.50(14)	C24	C22	C23	124.9(4)
C26	Ir1	C24	37.38(18)	C20	C22	Ir1	70.9(2)
C26	Ir1	C22	62.08(17)	C20	C22	C24	109.9(4)
C26	Ir1	C20	63.39(18)	C20	C22	C23	125.2(5)
C22	Ir1	C12	92.46(12)	C23	C22	Ir1	125.1(3)
C18	Ir1	C12	153.53(14)	C26	C18	Ir1	72.6(3)
C18	Ir1	C24	63.73(18)	C26	C18	C19	125.5(5)
C18	Ir1	C26	38.8(2)	C20	C18	Ir1	74.7(3)
C18	Ir1	C22	62.74(17)	C20	C18	C26	108.2(4)
C18	Ir1	C20	38.21(19)	C20	C18	C19	125.8(5)
C20	Ir1	C12	115.87(13)	C19	C18	Ir1	125.2(4)
C20	Ir1	C24	62.58(16)	C22	C20	Ir1	72.4(3)
C20	Ir1	C22	36.76(16)	C22	C20	C18	106.8(4)
C3	N4	C5	109.9(4)	C22	C20	C21	126.4(5)
C3	N4	C8	124.4(4)	C18	C20	Ir1	67.0(3)
C5	N4	C8	125.0(4)	C18	C20	C21	126.7(5)
C9	C10	Ir1	115.8(3)	C21	C20	Ir1	129.2(3)
C11	C10	Ir1	128.0(3)	C6	C5	N4	108.2(4)
C11	C10	C9	116.0(4)	C13	C14	C9	118.4(4)
N4	C3	Ir1	137.0(3)	C11	C12	C15	121.3(4)
N4	C3	N7	105.3(4)	C13	C12	C11	119.8(4)
N7	C3	Ir1	117.6(3)	C13	C12	C15	118.9(4)
C3	N7	C9	115.6(4)	O16	C15	C17	119.7(5)
C3	N7	C6	110.7(4)	O16	C15	C12	121.1(5)
C6	N7	C9	133.5(4)	C12	C15	C17	119.2(4)

C10	C9	N7	112.4(4)	C5	C6	N7	105.9(4)
C14	C9	C10	123.8(4)	C14	C13	C12	120.5(4)

Table S6 Hydrogen Atom Coordinates ( $\text{\AA} \times 10^4$ ) and Isotropic Displacement Parameters ( $\text{\AA}^2 \times 10^3$ ) for **3** (str1513).

Atom	x	y	z	U(eq)
H11	3411	4540	7480	29
H5	-4469	2964	9594	37
H23A	3928	1060	7525	56
H23B	2929	-321	7124	56
H23C	2854	384	8366	56
H17A	5030	5731	6192	71
H17B	5980	5910	7524	71
H17C	6461	6926	6732	71
H14	-572	6418	8504	35
H6	-2994	4941	9168	36
H13	1785	7561	7969	36
H8A	-3692	468	8589	52
H8B	-3501	998	9948	52
H8C	-1948	816	9447	52
H21A	2912	3247	5678	70
H21B	3181	2006	5121	70
H21C	4006	2586	6459	70
H25A	-131	-659	8430	65
H25B	-653	-1514	7176	65
H25C	-1934	-912	7678	65
H27A	-3517	19	6552	72
H27B	-3471	255	5233	72
H27C	-3424	1332	6235	72
H19A	-1684	2829	5215	84
H19B	-870	2259	4234	84
H19C	172	3424	5159	84

## Experimental

Single crystals of  $\text{C}_{22}\text{H}_{26}\text{ClIrN}_2\text{O}$  [**3**] were mounted on a MicroMount® polymer tip (MiteGen) in a random orientation. Data collection was performed on a SuperNova dual source equipped with a CCD Atlas detector diffractometer (Agilent Technologies). The crystal was kept at 200.00(10) K during data collection. Using Olex2 [1], the structure was solved with the ShelXS [2] structure solution program using Direct Methods and refined with the ShelXL [3] refinement package using Least Squares minimisation.

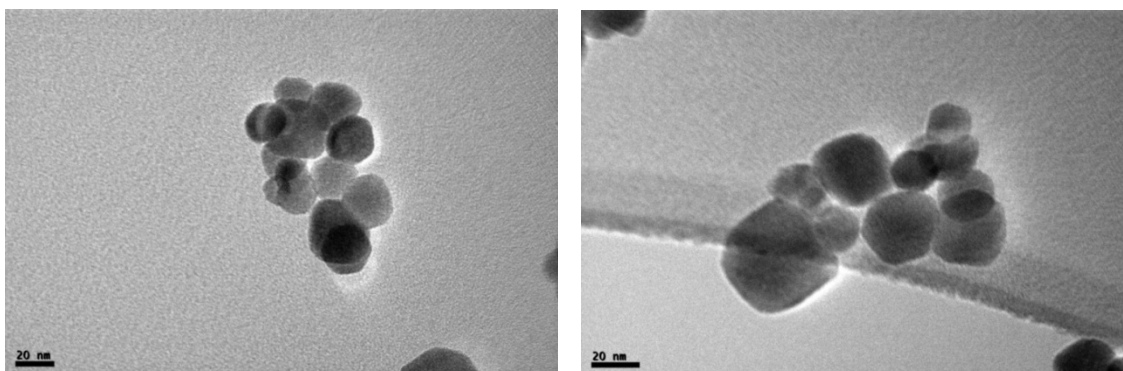


1. O. V. Dolomanov, L. J. Bourhis, R. J. Gildea, J. A. K. Howard and H. Puschmann, OLEX2: a complete structure solution, refinement and analysis program. *J. Appl. Cryst.* (2009). 42, 339-341.
2. SHELXS, G.M. Sheldrick, *Acta Cryst.* (2008). A64, 112-122
3. SHELXL, G.M. Sheldrick, *Acta Cryst.* (2008). A64, 112-122

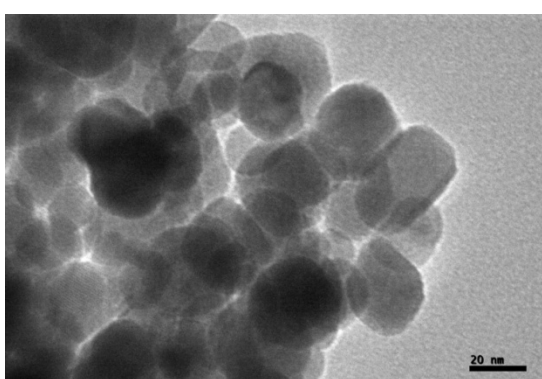
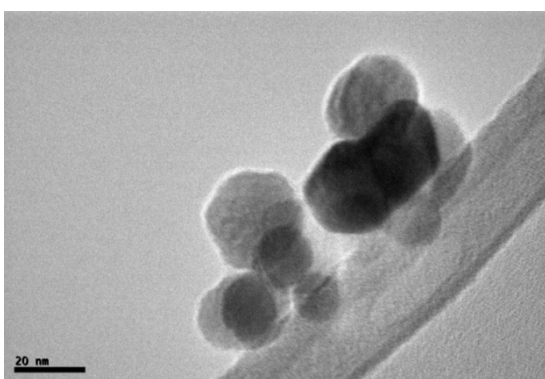
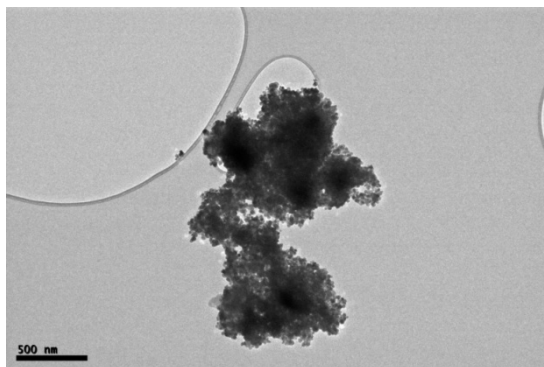
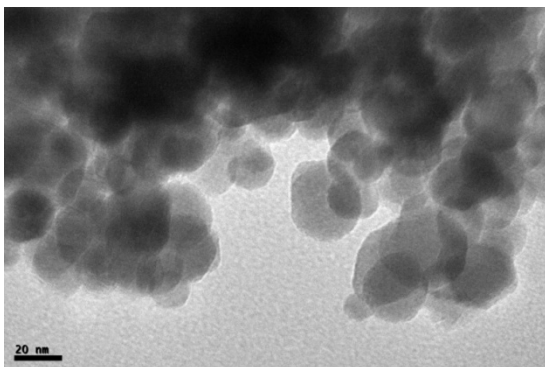
Crystal structure determination of **3** (str1513)

**Crystal Data** for  $C_{22}H_{26}ClIrN_2O$  ( $M=562.10$ ): triclinic, space group P-1 (no. 2),  $a = 8.4814(3) \text{ \AA}$ ,  $b = 11.4048(4) \text{ \AA}$ ,  $c = 11.4291(4) \text{ \AA}$ ,  $\alpha = 96.622(3)^\circ$ ,  $\beta = 99.334(3)^\circ$ ,  $\gamma = 104.274(3)^\circ$ ,  $V = 1043.17(6) \text{ \AA}^3$ ,  $Z = 2$ ,  $T = 200.00(10) \text{ K}$ ,  $\mu(\text{Cu K}\alpha) = 13.667 \text{ mm}^{-1}$ ,  $D_{\text{calc}} = 1.790 \text{ g/mm}^3$ , 19295 reflections measured ( $7.94 \leq 2\theta \leq 144.4$ ), 4047 unique ( $R_{\text{int}} = 0.0408$ ) which were used in all calculations. The final  $R_1$  was 0.0259 ( $>2\sigma(I)$ ) and  $wR_2$  was 0.0651 (all data).

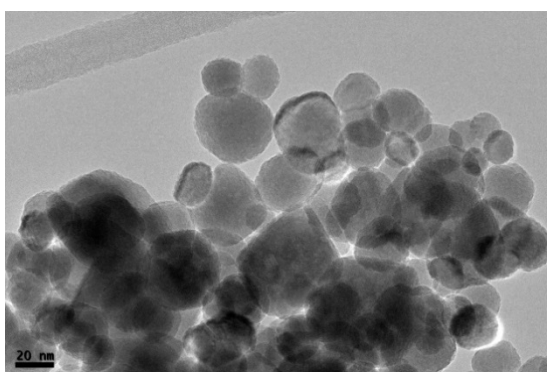
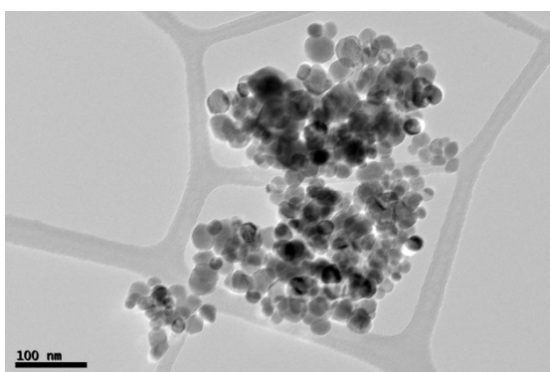
### S5.- High Resolution Transmission Electron Microscopy (HRTEM) Images



**Figure S1.** HRTEM images of commercial nano- $\text{Fe}_3\text{O}_4$



**Figure S2.** HRTEM images of nano-Fe<sub>3</sub>O<sub>4</sub>-dopa



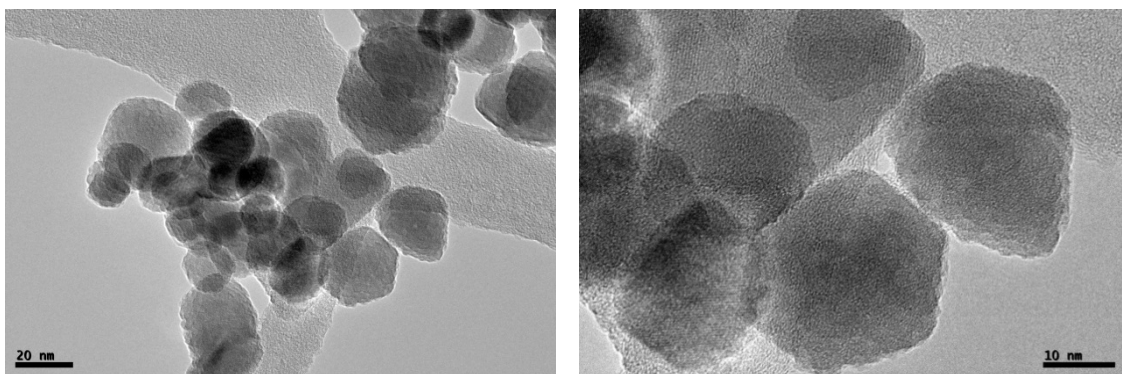


**Figure S3.** HRTEM images of nano-Fe<sub>3</sub>O<sub>4</sub>-dopa@Cp\*IrNHC (7)

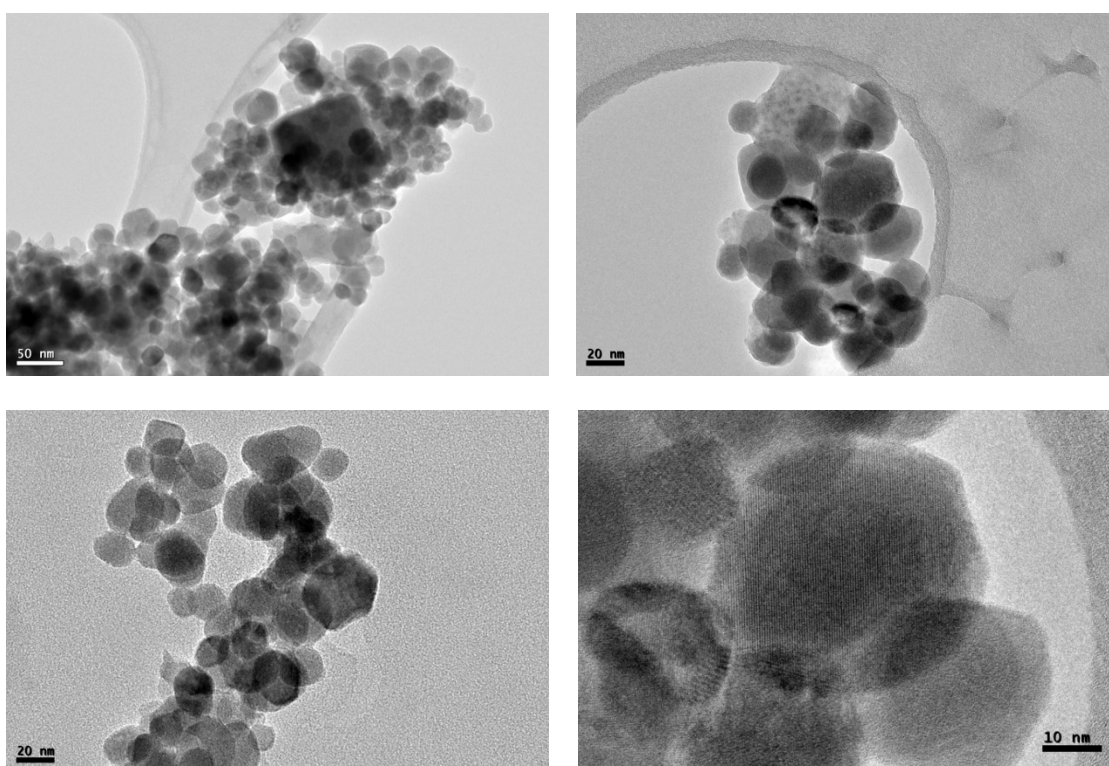


**Figure S4.** HRTEM images of nano-Fe<sub>3</sub>O<sub>4</sub>-dopa@Cp\*IrNHC (7) after three catalytic runs using acetophenone as substrate.

## S6.- FTIR Spectroscopy

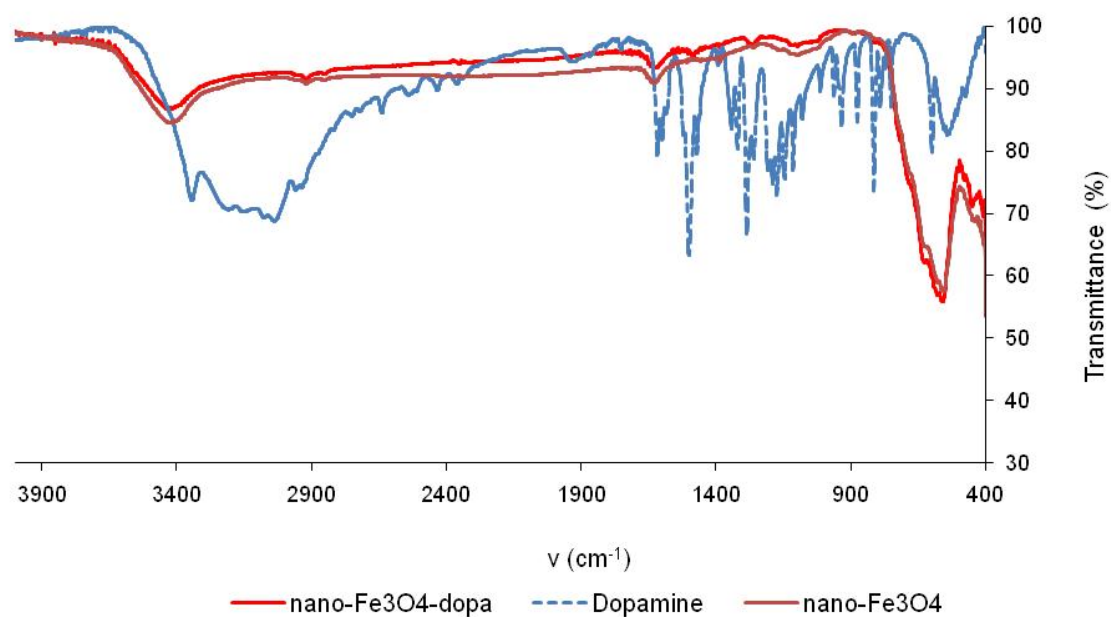


**Figure S5.** Comparative FTIR spectroscopic analysis of nano-Fe<sub>3</sub>O<sub>4</sub>-dopa, dopamine and nano-Fe<sub>3</sub>O<sub>4</sub>.

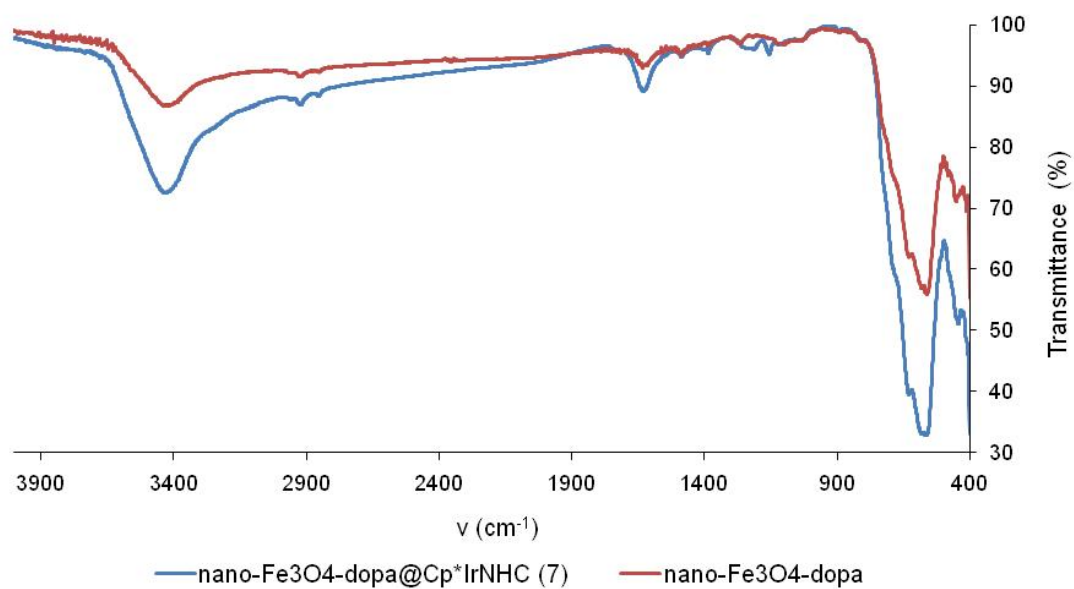


**Figure S6.** Comparative FTIR spectroscopic analysis of nano-Fe<sub>3</sub>O<sub>4</sub>-dopa@Cp\*IrNHC (7) and nano-Fe<sub>3</sub>O<sub>4</sub>-dopa.

### S7-. Powder XRD Studies

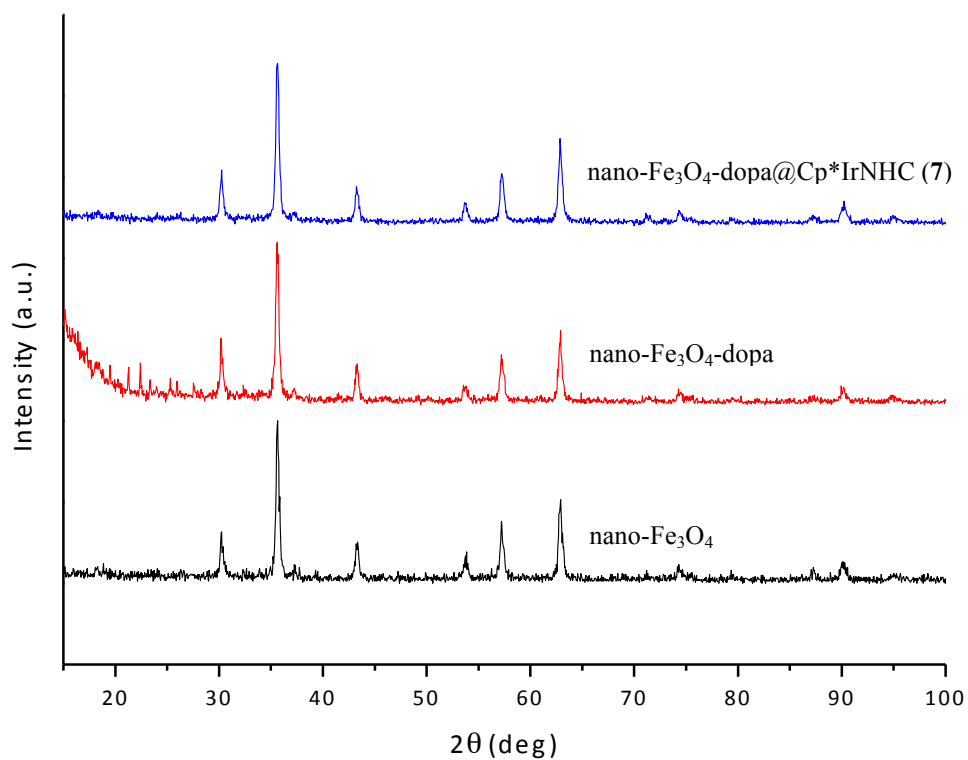


Figure S7. Powder XDR spectra of the materials

### S8.- Pictures of the catalyst separation

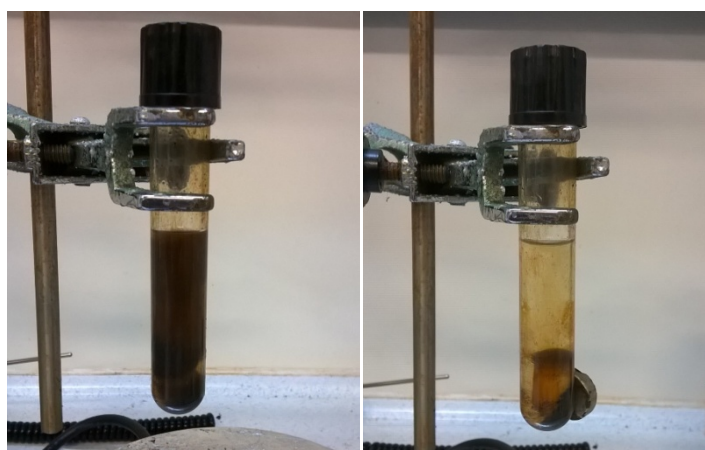
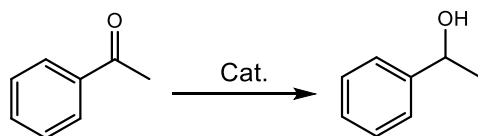
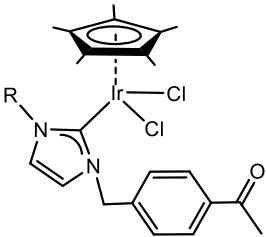
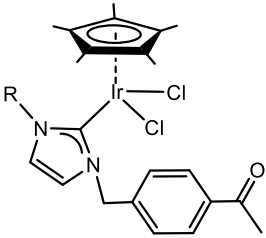
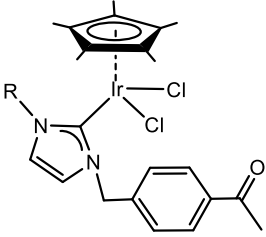
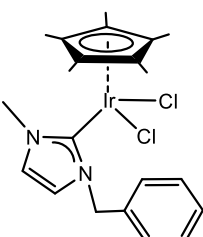
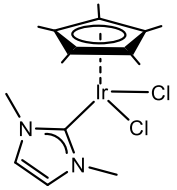
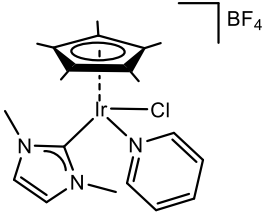
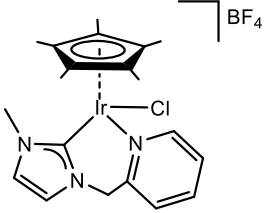
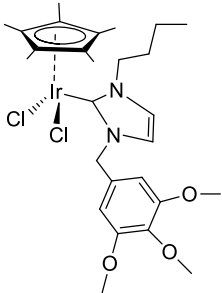
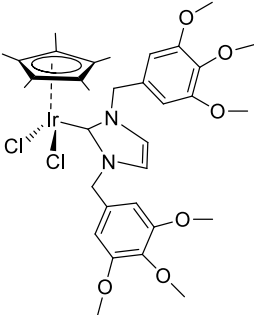
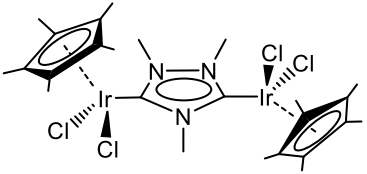
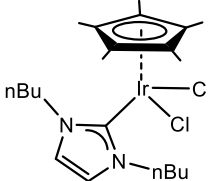
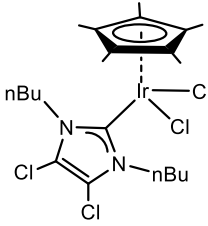
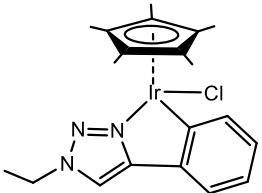
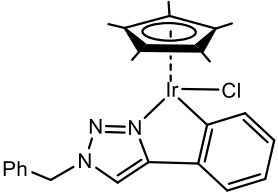


Figure S8. Catalyst recovery using an external magnet of nano-Fe<sub>3</sub>O<sub>4</sub>-dopa@Cp\*IrNHC.

**Table S7.** Comparative catalyst activity in the transfer hydrogenation of acetophenone

Entry	Catalyst	Conditions	Yield	Reference
1	 R = Methyl	<i>i</i> PrOH t-BuOK 82 °C 24 h Cat (0.5 mol%)	97	1
2	 R = 2,4,6-trimethylphenyl	<i>i</i> PrOH t-BuOK 82 °C 24 h Cat (0.5 mol%)	95	1
3	 R = acetylbenzyl	<i>i</i> PrOH t-BuOK 82 °C 24 h Cat (0.5 mol%)	96	1
4		<i>i</i> PrOH t-BuOK 82 °C 24 h Cat (0.5 mol%)	95	1

5		<i>i</i> PrOH KOH 82 °C 3 h Cat (1 mol%)	85	2
6		<i>i</i> PrOH KOH 82 °C 3 h Cat (1 mol%)	94	2
7		<i>i</i> PrOH KOH 82 °C 3 h Cat (1 mol%)	40	2
8		glycerol KOH 120 °C 7 h Cat (2.5 mol%)	35	3
9		glycerol KOH 120 °C 7 h Cat (2.5 mol%)	40	3

10		<i>i</i> PrOH Cs <sub>2</sub> CO <sub>3</sub> 100 °C 20 h Cat (2 mol%)	85	4
11		<i>i</i> PrOH AgOTf r.t. 8 h Cat (0.1 mol%)	50	5
12		<i>i</i> PrOH AgOTf r.t. 12 h Cat (0.1 mol%)	3	5
13		<i>i</i> PrOH KOH 100 °C 6 h Cat (0.5 mol%)	66	6
14		<i>i</i> PrOH KOH 100 °C 6 h Cat (0.5 mol%)	82	6



References:

1. X.-H. Zhu, L.-H. Cai, C.-X. Wang, Y.-N. Wang, X.-Q. Guo and X.-F. Hou, *J Mol Catal a-Chem*, 2014, **393**, 134.
2. U. Hintermair, J. Campos, T. P. Brewster, L. M. Pratt, N. D. Schley and R. H. Crabtree, *ACS Catal.*, 2014, **4**, 99.
3. A. Azua, J. A. Mata, E. Peris, F. Lamaty, J. Martinez and E. Colacino, *Organometallics*, 2012, **31**, 3911.
4. A. Zanardi, J. A. Mata and E. Peris, *J. Am. Chem. Soc.*, 2009, **131**, 14531.
5. R. Corberan and E. Peris, *Organometallics*, 2008, **27**, 1954.
6. R. Maity, S. Hohloch, C.-Y. Su, M. van der Meer and B. Sarkar, *Chem. Eur. J.*, 2014, **20**, 9952.